

Fission in a wall-and-window one-body-dissipation model

Arnold J. Sierk and J. Rayford Nix

Theoretical Division, Los Alamos Scientific Laboratory, University of California, Los Alamos, New Mexico 87545

(Received 5 October 1979)

We calculate the fission of idealized nuclei in a modified liquid-drop model. The potential energy is taken to be a combination of Coulomb energy and nuclear energy obtained by double folding a Yukawa-plus-exponential two-body potential. The collective nuclear kinetic energy is calculated by use of the Werner-Wheeler approximation to incompressible, irrotational flow. The dissipation of collective energy into internal energy is calculated from the one-body wall formula until the neck decreases to a critical size, at which point a transition is made to a combination of the one-body wall formula relative to the centers of mass of the two nascent fragments and the one-body window formula. Experimental fission-fragment kinetic energies for the fission of nuclei throughout the Periodic Table are reproduced optimally when the neck radius at the transition point is 2.5 fm. For the alternative dissipation mechanism of ordinary two-body viscosity, the experimental fission-fragment kinetic energies are reproduced equally well when the viscosity coefficient is 0.015 TP.

NUCLEAR REACTIONS, FISSION ^{236}U , nuclei throughout Periodic Table; calculated most probable fission-fragment kinetic energies. Modified liquid-drop model, Yukawa-plus-exponential potential, one-body dissipation, wall formula, window formula, two-body viscosity.

I. INTRODUCTION

One of the interesting questions in nuclear physics is the dynamical nature of large-scale collective motions, such as those that occur during fission and nonperipheral heavy-ion collisions. While it is possible to explain some of the observed features of such reactions using a viscous liquid-drop model,^{1,2} there is strong reason to believe that a hydrodynamical model, based on the assumption of a short mean free path between two-nucleon collisions, is inappropriate for nuclei. Because the Pauli exclusion principle forbids scattering into occupied states, the mean free path between two-nucleon collisions is expected to be larger than the size of the nucleus. Therefore, there is some reason to expect that the dominant process in collective motion of nuclei is one-body dynamics, or the interactions between individual nucleons and the mean field created by all the other nucleons.³ However, the apparent dominance of one-body effects does not necessarily imply that two-body collisions should be totally ignored, as they can still significantly perturb the situation from an ideal one-body limit.

One macroscopic approximation to the one-body dynamical problem is to use the wall formula to describe the dissipation.³ If one assumes that the particles hitting the boundaries of the mean field have velocities isotropically distributed around an average drift velocity of the nucleus, then any motion of the mean-field wall relative to the drift velocity leads to a loss of energy to the particles inside the mean field at the rate³

$$\frac{dE}{dt} = \rho \bar{v} \oint \dot{n}^2 dS, \quad (1)$$

where ρ is the mass density of the nucleus, \bar{v} is the average nucleon speed relative to the drift velocity, \dot{n} is the relative normal velocity of the wall with respect to the drift velocity of the system, and the integral is over the entire boundary or wall of the system. This wall formula, with values of ρ and \bar{v} appropriate to nuclei, implies such a high rate of dissipation that inertial effects are unimportant, and a creeping type of motion results.³

An important difficulty in applying Eq. (1) to nuclei is the assumption of isotropy of particle motion with respect to the drift velocity of the nucleus. There are at least two distinct problems to consider. First, the assumption is obviously not satisfied for a nucleus during fission just after scission, where a blind application of the wall formula would predict that the fragment separation would be strongly damped, leading to no fragment kinetic energy. In the case of separated fragments, one should obviously apply the wall formula to each fragment individually.³ However, it is more difficult to decide how to make the transition before scission, when the nucleus is highly deformed and the particles striking the walls are not moving isotropically with respect to the center of mass of the nucleus.⁴

The second problem is related to the question of reversibility. The energy dissipated through the wall formula is actually into zero-sound energy (distortion of the Fermi surface). Thus, the velocity distribution striking some portion of the

wall at a given time will not be isotropic due to wall motion at other places at earlier times. This change in shape of the velocity distribution of particles hitting the wall will lead to a very different dissipation rate and in some cases will couple energy from zero sound back to collective or wall motion. In a highly symmetric situation, the net rate of energy loss may be drastically reduced^{3,5} from that predicted by Eq. (1).

In this paper we consider only the first problem, modifying the wall formula for fissioning nuclei when their shapes become highly deformed. We discuss the model that we use in Sec. II and present our calculated results in Sec. III. In Sec. IV we give a summary and discussion of our results.

II. WALL-AND-WINDOW MODEL

Another simplification of one-body dynamics arises when there are two almost separate systems connected by a small window, such as nascent fission fragments or colliding ions.³ If the two systems are in relative motion, any particles passing through the window will damp the motion because of the momentum transferred between the systems. If we define the relative velocity of the two systems as \tilde{u} and the area of the window between them as $\Delta\sigma$, then the dissipation rate is³

$$\frac{dE}{dt} = \frac{1}{4}\rho\bar{v}\Delta\sigma(2u_{\parallel}^2 + u_{\perp}^2), \quad (2)$$

where u_{\parallel} is the component of \tilde{u} along the normal to the window and u_{\perp} is the component of \tilde{u} in the plane of the window.

Since we are unable to calculate the velocity distribution on the entire wall as a function of time, we investigate a much simpler model. We assume wall-formula dissipation until the neck is smaller than a critical size, at which point we switch to window dissipation for the relative motion of the two ends, with wall dissipation applying for motions of the fragment walls relative to their respective centers of mass.

We consider axially symmetric shapes described in cylindrical coordinates by a surface function

$$\rho_s = \rho_s(q, z),$$

where $q = \{q_i\}$ denotes a set of collective coordinates. The quantity \hat{n} entering the wall formula is then

$$\begin{aligned} \hat{n} &\equiv \tilde{v}_s \cdot \hat{n} = \frac{\partial \rho_s}{\partial t} \left[1 + \left(\frac{\partial \rho_s}{\partial z} \right)^2 \right]^{-1/2} \\ &= \sum_i \dot{q}_i \rho_s \frac{\partial \rho_s}{\partial q_i} \left[\rho_s^2 + \left(\rho_s \frac{\partial \rho_s}{\partial z} \right)^2 \right]^{-1/2}, \end{aligned}$$

where \hat{n} is the outward unit normal to the surface and \tilde{v}_s is the velocity on the surface.

The dissipation tensor η_{ij} is defined by

$$\frac{dE}{dt} = \sum_{i,j} \eta_{ij} \dot{q}_i \dot{q}_j.$$

For the wall formula, it is therefore given by

$$\eta_{ij} = \frac{\pi\rho\bar{v}}{2} \int_{z_{\min}}^{z_{\max}} dz \frac{\partial \rho_s^2}{\partial q_i} \frac{\partial \rho_s^2}{\partial q_j} \left[\rho_s^2 + \frac{1}{4} \left(\frac{\partial \rho_s^2}{\partial z} \right)^2 \right]^{-1/2}. \quad (3)$$

For wall-and-window dissipation applied to a reflection-symmetric shape, we must replace \hat{n} in Eq. (1) by $\hat{n} \cdot (\tilde{v}_s - \frac{1}{2}\dot{R}\hat{e}_z)$, where \hat{e}_z is the unit vector along the axis of symmetry and \dot{R} is the relative velocity of the centers of mass of the two halves of the fissioning drop. In addition, we must add to dE/dt a term of the form $\eta_{\text{window}}\dot{R}^2$, which can be calculated from Eq. (2). This leads to

$$\begin{aligned} \eta_{ij} &= \frac{1}{2}\rho\bar{v} \left\{ \frac{\partial R}{\partial q_i} \frac{\partial R}{\partial q_j} \Delta\sigma + \pi \int_{z_{\min}}^{z_{\max}} dz \left(\frac{\partial \rho_s^2}{\partial q_i} - \frac{1}{2} \frac{\partial \rho_s^2}{\partial z} \frac{\partial R}{\partial q_i} \right) \right. \\ &\quad \times \left(\frac{\partial \rho_s^2}{\partial q_j} - \frac{1}{2} \frac{\partial \rho_s^2}{\partial z} \frac{\partial R}{\partial q_j} \right) \\ &\quad \left. \times \left[\rho_s^2 + \left(\frac{1}{4} \frac{\partial \rho_s^2}{\partial z} \right)^2 \right]^{-1/2} \right\} \quad (4) \end{aligned}$$

for the wall-and-window model.

The Rayleigh dissipation function F is defined by

$$F \equiv \frac{1}{2} \frac{dE}{dt} = \frac{1}{2} \sum_{i,j} \eta_{ij} \dot{q}_i \dot{q}_j,$$

and the collective kinetic energy T is defined by

$$T = \frac{1}{2} \sum_{i,j} M_{ij} \dot{q}_i \dot{q}_j,$$

where M_{ij} is the inertia tensor. With the collective potential energy denoted by $V(q)$ and the Lagrangian defined by $L = T - V$, the modified Lagrange equations of motion¹

$$\frac{d}{dt} \left(\frac{\partial L}{\partial \dot{q}_i} \right) - \frac{\partial L}{\partial q_i} = - \frac{\partial F}{\partial \dot{q}_i} \quad (5)$$

then determine classically the dynamical evolution of the nuclear shape.

We parametrize our shapes as two end spheroids smoothly joined to a third spheroid or to a hyperboloid of revolution of one sheet.⁶ For reflection-symmetric shapes this parametrization has three independent collective coordinates. The collective potential energy is taken to be the sum of the Coulomb electrostatic energy of a uniform-charge-density drop and a nuclear macroscopic energy obtained by double folding a Yukawa-plus-exponential two-body potential over the volume of the drop.^{7,8} This form of nuclear macroscopic energy, while exhibiting some of the same properties as that calculated by double folding a single Yukawa function,⁹ is better because it exhibits saturation and properly represents the tail of the

internuclear potential measured in heavy-ion elastic scattering experiments.⁸ The collective kinetic energy is calculated by use of the Werner-Wheeler approximation^{1,6} to incompressible, irrotational flow.

For displaying the dynamical paths of fissioning nuclei it is convenient to project the results out of the multidimensional space spanned by the $\{q_i\}$ onto the subspace spanned by the two most important symmetric degrees of freedom. These are defined in terms of the central moments¹

$$r \equiv 2\langle z \rangle$$

and

$$\sigma \equiv 2\langle (z - \langle z \rangle)^2 \rangle^{1/2},$$

where the brackets $\langle \rangle$ denote an average over the half volume to the right of the midplane of the reflection-symmetric shape.

III. CALCULATED RESULTS

We solve Eq. (5) for initial conditions corresponding to the most probable path, in which the nucleus is started from rest an infinitesimal distance in the fission direction beyond the fission saddle point. The calculation proceeds until a shape with zero neck radius is reached, at which point the postscission motion of the fragments is approximated by constraining them to be spheroids with aligned symmetry axes.¹

In Fig. 1 we show the projection onto the space of central moments r and σ of the most probable fission paths for ^{236}U for various dissipation mo-

del. The lowest dashed curve gives the trajectory for no dissipation. Increasing ordinary hydrodynamical shear viscosity results in a more elongated scission configuration, since elongation is damped less than neck formation with this type of dissipation.¹ The lowest solid curve gives the trajectory for the wall-formula one-body dissipation. The motion leads to a more compact configuration, since wall-formula dissipation hinders elongation more strongly than it does neck formation.³ The motion is so strongly damped that the scission point is reached with less than 1 MeV of translational kinetic energy in the system. The Coulomb energy of the compact configuration is high enough to lead to a final fragment kinetic energy that is approximately equal to that for the $\mu = 0.015$ TP two-body-viscosity case. In this latter case, the scission shape is more elongated, but it also has about 20 MeV of translational kinetic energy.

When implementing the wall-and-window approach, we follow the wall-formula dynamical path to a point where the radius of the neck is less than a critical value. We then switch from Eq. (3) to Eq. (4) to describe the dissipation tensor, using this latter form until the neck radius goes to zero. The postscission model in both cases is the wall formula applied to each fragment, since the window friction is zero between the fragments. Because the wall-and-window model damps elongation much less strongly than does the pure wall formula, the precission trajectories extend to larger values of r and σ . If the transition is made when the neck is cylindrical, which is very nearly at the saddle point for ^{236}U , the shape of the trajectory in r - σ space is almost the same as for the case of no dissipation. However, the dynamical evolution is substantially different in these two cases. For example, there is about 10 MeV of kinetic energy at scission for the case of wall-and-window dissipation, whereas there is about 30 MeV with no dissipation.

As the transition is made for successively smaller necks, the trajectories branch off from the wall-formula trajectory farther along, leading to increasingly less elongation at scission. We show in Fig. 2 how the calculated fission-fragment kinetic energy varies with the radius of the neck at which the transition is made. For the pure wall formula the kinetic energy is about 170 MeV, which is nearly all Coulomb-plus-nuclear interaction energy of the fragments at scission. For a small value of the transition neck radius, the system begins to acquire some translational kinetic energy at scission without becoming so elongated as to lose much Coulomb energy. Therefore, the initial effect of increasing the transition neck

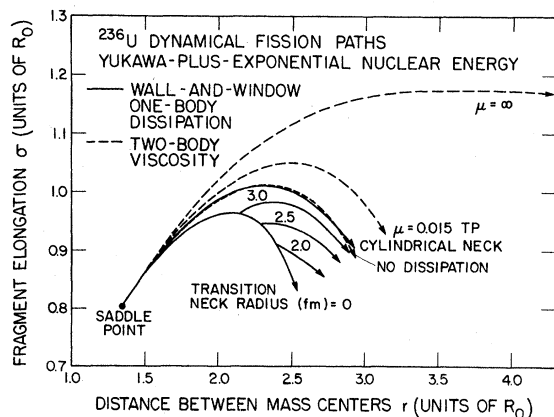


FIG. 1. Most probable dynamical trajectories in r - σ space for the fission of ^{236}U for various types of dissipation. The dashed curves are trajectories for either no dissipation or two-body viscosity, whereas the solid curves are trajectories for one-body wall-formula dissipation with a transition to wall-and-window dissipation at the indicated neck radii.

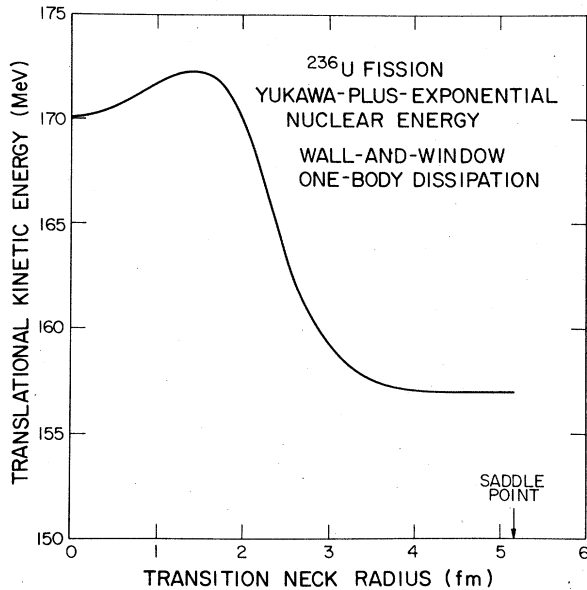


FIG. 2. Calculated fission-fragment kinetic energy for the fission of ^{236}U as a function of the neck radius at which a transition is made between the wall formula and the wall-and-window formula.

radius is to increase the kinetic energy somewhat. However, as the transition neck radius is increased further, the scission shape becomes more elongated, leading to a decrease in Coulomb interaction energy that is no longer totally compensated for by increased translational kinetic energy at scission. The calculated fragment kinetic energy decreases to 157 MeV when the wall-and-window dissipation is used for the entire dynamical evolution. These energies are to be compared to the experimental most probable fission-fragment kinetic energy¹⁰ of 168.0 ± 4.5 MeV for the fission of ^{236}U at high excitation energy, where single-particle effects are substantially reduced.

We have performed similar calculations for nuclei along Green's approximation to the valley of β stability.¹¹ We compare these calculated fission-fragment kinetic energies to experimental data in Fig. 3. The simple wall formula, with no adjustable parameters, satisfactorily reproduces the experimental data. However, as seen from the figure, the experimental data are reproduced slightly better when the transition to wall-and-window dissipation occurs at a neck radius of about 2.5 fm.

We present in the Appendix similar calculations using ordinary two-body viscosity, which differ from the calculations in Ref. 1 by including the nuclear macroscopic energy calculated using the Yukawa-plus-exponential two-body potential.^{7,8}

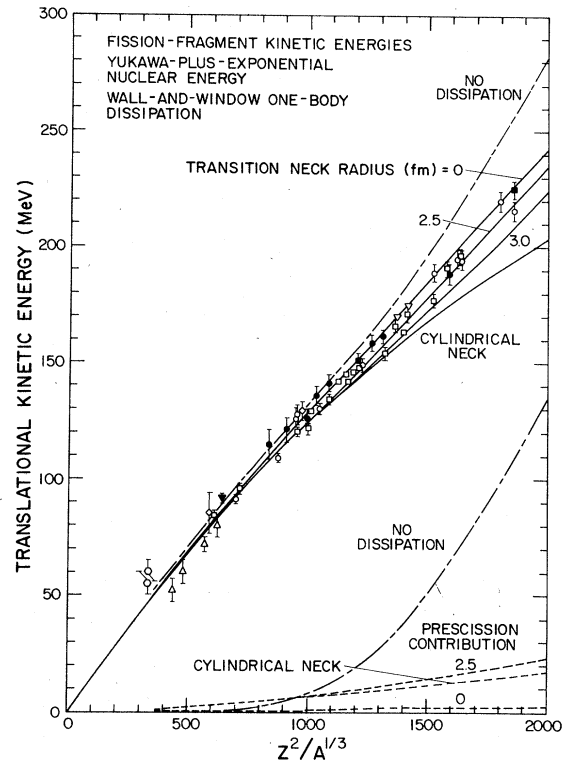


FIG. 3. Comparison of experimental most probable fission-fragment kinetic energies with results calculated for wall-and-window dissipation with different transition neck radii. The experimental data are for the fission of nuclei at high excitation energies, where the most probable fission-fragment mass distribution is into two equal fragments. The open symbols represent values for equal mass divisions only, whereas the solid symbols represent values averaged over all mass divisions. The origins of the experimental data are given in Ref. 1. The dashed curves give the calculated translational kinetic energies at the scission point.

IV. SUMMARY AND CONCLUSIONS

We have calculated the fission of nuclei throughout the Periodic Table by use of a modified-liquid-drop model, with dissipation included by means of two approximations to the extreme one-body-dynamics limit. The wall-formula approximation, in which the collective energy is assumed to be dissipated irreversibly into distortions of the Fermi surface, predicts correctly the observed most probable fission-fragment kinetic energies. Modification of the assumption of isotropic particle velocities leads to another approximate model of one-body dynamics. In the wall-and-window approximation, the motion of the centers of mass of two ions or nascent fission fragments is damped by the momentum transfer caused by single par-

ticles passing through the window between the two fragments. Distortions of the fragments are damped by applying the wall formula relative to the centers of mass of the fragments. This model reproduces the experimentally observed fission-fragment kinetic energies slightly better when the transition from wall to wall-and-window dissipation occurs at a neck radius of about 2.5 fm.

By making this abrupt transition, we hope to crudely approximate the continuous transition from an isotropic velocity distribution to one in which the particles in one fragment have an average velocity different from that of the particles in the other fragment. These two models, although giving similar results for fission-fragment kinetic energies, should give very different predictions for angular distributions and possibly for final kinetic energies in heavy-ion collisions.

Both of these models, however, neglect one effect that can be extremely important for collective motions with high symmetry. In a realistic model of one-body dynamics, some of the energy coupled to zero sound will reappear in the collective motion, leading to a very different dynamical picture than that presented here. For example, in one model of giant multipole resonances, the one-body dynamics, instead of giving an extremely large damping, provides the basic restoring force which makes the resonances possible.¹²⁻¹⁵ The forces due to one-body effects are large in both pictures, but a difference in phase changes a large dissipative force into a large conservative force.⁵ Therefore, we feel that one should be very cautious about interpreting results of calculations using very simplified approximations to one-body-dominated collective dynamics.

We are grateful to W. J. Swiatecki for conversations that stimulated the calculations reported in this paper.

APPENDIX: FISSION CALCULATED WITH TWO-BODY VISCOSITY

We present here the results of calculations of fission-fragment kinetic energies using two-body

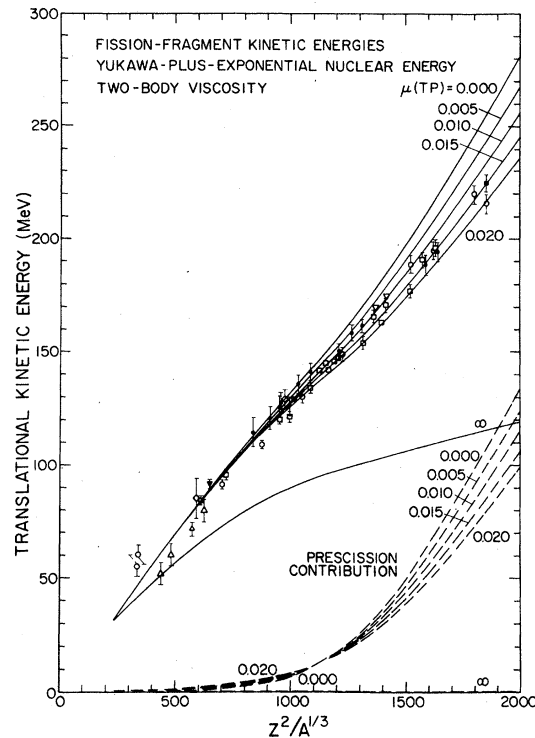


FIG. 4. Similar to Fig. 3, with the dissipation given by ordinary two-body viscosity.

viscosity as the dissipation mechanism. These calculations are similar to those in Ref. 1, but differ by the use here of the Yukawa-plus-exponential nuclear macroscopic energy.^{7,8} We show in Fig. 4 the calculated fission-fragment kinetic energies for nuclei throughout the Periodic Table for several values of the two-body viscosity coefficient. A value of $\mu = 0.015$ TP satisfactorily reproduces the experimental data. The unit of viscosity is the terapoise, which is given by

$$1 \text{ TP} = 10^{12} \text{ P} = 10^{12} \text{ dyn s/cm}^2 \\ = 6.24 \times 10^{-22} \text{ MeV s/fm}^3 = 0.948 \hbar/\text{fm}^3.$$

¹K. T. R. Davies, A. J. Sierk, and J. R. Nix, Phys. Rev. C **13**, 2385 (1976).

²A. J. Sierk and J. R. Nix, in Proceedings of the Symposium on Macroscopic Features of Heavy-Ion Collisions, Argonne, Illinois, 1976, Argonne National Laboratory Report No. ANL/PHY-76-2, 1976 (unpublished), p. 407.

³J. Błocki, Y. Boneh, J. R. Nix, J. Randrup, M. Robel, A. J. Sierk, and W. J. Swiatecki, Ann. Phys. (N. Y.)

113, 330 (1978).

⁴A. J. Sierk, S. E. Koonin, and J. R. Nix, Phys. Rev. C **17**, 646 (1978).

⁵J. R. Nix and A. J. Sierk, in Proceedings of the Topical Conference on Large Amplitude Collective Nuclear Motion, Keszthely, Lake Balaton, Hungary, 1979 (to be published).

⁶J. R. Nix, Nucl. Phys. **A130**, 241 (1969).

⁷H. J. Krappe, J. R. Nix, and A. J. Sierk, Phys. Rev.

- Lett. 42, 215 (1979).
- ⁸H. J. Krappe, J. R. Nix, and A. J. Sierk, Phys. Rev. C 20, 992 (1979).
- ⁹H. J. Krappe and J. R. Nix, in *Proceedings of the Third International Atomic Energy Agency Symposium on the Physics and Chemistry of Fission, Rochester, New York, 1973* (International Atomic Energy Agency, Vienna, 1974), Vol. I, p. 159.
- ¹⁰D. S. Burnett, Lawrence Berkeley Laboratory Report No. UCRL-11006, 1963 (unpublished).
- ¹¹A. E. S. Green, *Nuclear Physics* (McGraw-Hill, New York, 1955), pp. 185, 250.
- ¹²G. F. Bertsch, Nucl. Phys. A249, 253 (1975).
- ¹³J. P. Blaizot, Phys. Lett. 78B, 367 (1978).
- ¹⁴H. Sagawa and G. Holzwarth, Prog. Theor. Phys. 59, 1213 (1978).
- ¹⁵J. R. Nix and A. J. Sierk, Phys. Rev. C 21, 396 (1980).